Preliminary Simulation of Aerosol Dynamics in the Cover Gas Region of the PGSFR

Dehee Kim [a*], Jonggan Hong [a], Jaehyuk Eoh [a]
[a]*Korea Atomic Energy Research Institute, 111 Daedeok-daero 989beon-gil, Yuseong-gu, Daejeon, Korea*
[*]*Corresponding author: dehee@kaeri.re.kr*

1. Introduction

The cover gas region of PGSFR (Prototype Gen-IV Sodium-cooled Fast Reactor) is filled with argon gas. From the free surfaces of hot and cold sodium pools, sodium vapor is generated by molecular diffusion and mixed into the cover gas. Sodium aerosol is produced by nucleation and grown into various sizes of aerosols by condensation and agglomeration. The sodium aerosols float inside the cover gas region by natural convection and deposit on the structures or settle down on the sodium free surfaces.

It was reported that the sodium aerosol deposition on the surfaces of components might affect the heat transfer characteristics to the structures and hinder the operation of the instruments installed in the cover gas region [1]. Therefore, it is necessary to figure out the aerosol dynamics inside the cover gas region.

In this work, aerosol behavior inside the cover gas region of the PGSFR is simulated preliminarily using an OpenFOAM solver, 'aerosolEulerFoam' [2]. The solver is validated for a natural convection case and applied for a simulation of aerosol motion in the cover gas region.

2. Methods and Results

General dynamic equation (GDE) describes the transient variation of particle concentration which is influenced by nucleation, condensation, agglomeration, diffusion, and so on. GDE can be solved by sectional method or moment method. The 'aerosolEulerFoam' is utilizing the Eulerian approach to solve fluid flow and solving the GDE with sectional and moment methods. Aerosol deposition is result of gravitational sedimentation, Brownian/turbulent diffusion, drift, and thermophoresis.

2.1 Governing equations

Continuity, momentum, energy, number density, and mass fraction equations are written as follows [2].

$$\partial_t \rho + \nabla \cdot (\rho \boldsymbol{u}) + \nabla \cdot [\boldsymbol{f}(1-\gamma)] = 0, \quad (1)$$

$$\partial_t (\rho \boldsymbol{u}) + \nabla \cdot (\rho \boldsymbol{u}\boldsymbol{u}) = -\nabla p - \nabla \cdot \boldsymbol{\tau}, \quad (2)$$

$$c_p[\partial_t(\rho T) + \nabla \cdot (\rho \boldsymbol{u} T)] = \nabla \cdot (k \nabla T) - (\boldsymbol{\tau} : \nabla \boldsymbol{u}) + D_t p, \quad (3)$$

$$\partial_t (\rho M_i) + \nabla \cdot (\rho \boldsymbol{u} M_i) + \nabla \cdot \left(\rho \boldsymbol{u}_i^p M_i\right) = \nabla \cdot \left(D_i^p \nabla \rho M_i\right) + J_{M_i}, \quad (4)$$

$$\partial_t \left(\rho Y_j\right) + \nabla \cdot \left(\rho \boldsymbol{u} Y_j\right) - \nabla \cdot \left(Y^{-1} \boldsymbol{h} Y_j\right) = R_j, \quad (5)$$

$$\partial_t \left(\rho Z_j\right) + \nabla \cdot \left(\rho \boldsymbol{u} Z_j\right) - \nabla \cdot \left(Z^{-1} \boldsymbol{f} Z_j\right) = S_j, \quad (6)$$

$\boldsymbol{u}, \rho, \boldsymbol{f}, \gamma$ denote velocity, density of component mixture, total flux of particle concentration drifting away from the mixture motion, and ratio between local vapor density and local particle density, respectively. p is static pressure and $\boldsymbol{\tau}$ is defined as $\boldsymbol{\tau} = -\mu[\nabla \boldsymbol{u} + (\nabla \boldsymbol{u})^T] + \frac{2}{3}\mu(\nabla \cdot \boldsymbol{u})\boldsymbol{I}$. μ is dynamic viscosity. k, c_p are thermal conductivity and specific heat, respectively.

$M_i, \boldsymbol{u}_i^p, D_i^p, J_{M_i}$ are aerosol number density divided by density, particle velocity, particle diffusion coefficient, source term related with nucleation and condensation, respectively. The subscript i is used to denote a section index for the representative aerosol size group.

$Y_j, Z_j, \boldsymbol{h}, R_j, S_j$ are vapor mass fraction, particle mass fraction, vapor mass concentration drift flux ($\boldsymbol{h} = \gamma \boldsymbol{f}$), vapor and particle mass concentration source terms, respectively.

2.2 Brownian diffusion model

Diffusion flux $\boldsymbol{f}^{\text{diff}}$ mainly depends on D_i^p. A model for the Brownian diffusivity for a sphere body [2] is given by

$$D^p(s) = \frac{k_B T C_c}{3\pi\mu d}, \quad (7)$$

where, k_B, C_c, d denote the Boltzmann constant, Cunningham correction factor, and aerosol diameter, respectively. Cunningham correction factor accounts for surface slip of small particles.

2.3 Drift model

Schiller-Naumann model [2] to calculate drift velocity of a particle is written as

$$\partial_t \boldsymbol{v}(\mathrm{s}) + [\boldsymbol{v}(\mathrm{s}) \cdot \nabla]\boldsymbol{v}(\mathrm{s}) = -\frac{1+0.15 Re_d^{0.687}}{\tau}[\boldsymbol{v}(\mathrm{s}) - \boldsymbol{u}] + (1-\gamma)\mathbf{g}, \quad (8)$$

where, $\boldsymbol{v}, \tau, \mathbf{g}$ are particle velocity, particle relaxation time, gravitational acceleration, respectively. τ is defined as $\tau = \rho^p d^2/(18\mu)$ and Re_d is a function of $\boldsymbol{v}$.

2.4 Thermophoresis model

In a flow region with a temperature gradient, especially near the structure surfaces, thermophoretic force is acting on particles. The thermophoretic force is expressed as [3]

$$F_T = -\frac{6\pi\mu v d_p C_s}{1+3C_m Kn}\frac{\frac{k_g}{k_p}+C_t Kn}{1+2\frac{k_g}{k_p}+2C_t Kn}\frac{\nabla T}{T}, \quad (9)$$

where, $C_s, C_m, C_t, Kn, k_g, k_p$ denote thermal slip coefficient, velocity slip coefficient, thermal jump coefficient, Knudsen number, thermal conductivity of gas, and thermal conductivity of particle, respectively.

2.5 Validation for natural convection

The OpenFOAM solver was validated for a natural convection case. A closed square box has different temperatures for side walls. Temperature difference between two walls was set to 10K and other parameters are given to set Ra number to be 10^5. Left wall is hot and right wall cold. 80x80 grid system stretched on to the walls was generated as in Figure 1.

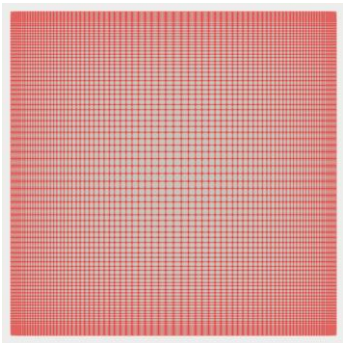

Fig. 1. Grid system for natural convection

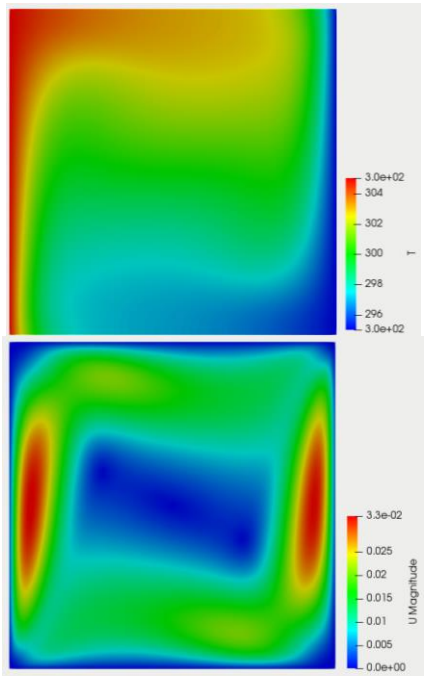

Fig. 2. Temperature (top) and velocity (bottom) contours of natural convection

Figure 2 displays temperature and velocity contours. From the left wall, the fluid goes up by buoyant force and goes down at the right wall due to cold wall. Average Nusselt number at the left wall was calculated as 4.5261 which is very similar to the value of 4.5231 for which 320x320 grid system was used [4].

2.6 Simulation of aerosol behavior in the cover gas region

The reactor structure of the PGSFR is shown in Fig. 3 in which cover gas region is displayed as green color. Thermo-hydraulic characteristics incorporating the reactor vessel, the reactor vault cooling system, and the head access area was analyzed by a coupled simulation [5]. Temperatures at the reactor vessel, the reactor head, the pumps, the heat exchangers, the upper shield structure, and the redan are required for a cover gas region simulation. Therefore, the boundary conditions were extracted from the simulation result [5].

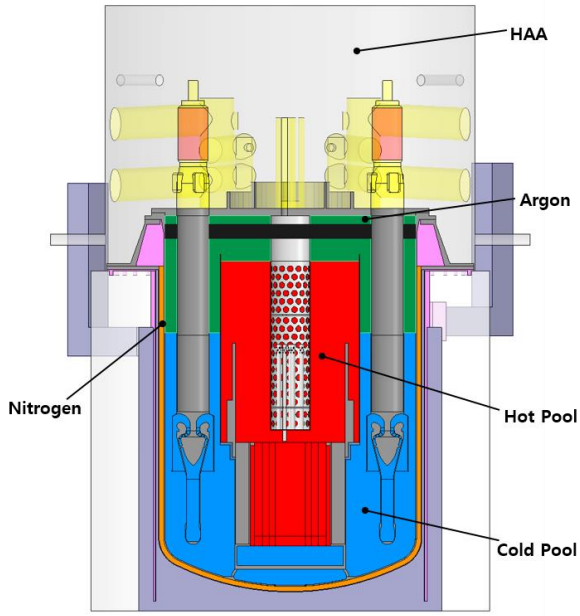

Fig. 3. Cover gas region (argon, green color) in the PGSFR

Only the argon region was simulated and the full computational domain is shown in Fig. 4. In Figs. 5 and 6, temperature and velocity distributions are displayed. Temperatures of the structures range between 540℃ of the hot pool and about 150℃ of the reactor head. Around the redan, velocity magnitude is high. Temperature of the cover gas region under the upper shield structure is high compared to that of the cover gas region above the upper shield structure. The hot sodium vapor is transported to the upper region passing through the narrow gap between the upper shield structure and the reactor vessel. Counter mean diameter at a horizontal section is displayed in Fig. 7. At the lower temperature region around the narrow gap, aerosol size is bigger than the other space which show possibility of aerosol growth near the reactor vessel in the upper cover gas region. If the aerosols grow and agglomerate more and more in the region, there is a possibility of small blockage in the gap

which is about 13 mm. By the way, an inert gas purification system is mounted on the reactor head and the inflow and outflow of the system can affect the aerosol behavior.

In this preliminary study, deposition amount on the structures was not calculated but it is required of further study for the influence of the aerosol deposition for the heat transfer to the structures and the operation of the instruments.

3. Conclusions

Sodium aerosol in the cover gas region was simulated and the aerosol growth was shown near the narrow gap. The aerosol growth and deposition can affect flow characteristics of the upper cover gas region and the heat transfer to the structures and the operation of the instruments in the cover gas region. Therefore, more specific simulation is required to investigate the aerosol transport features reflecting on an inert gas purification system installed in the cover gas region.

ACKNOWLEDGEMENT

This work was supported by the National Research Foundation of Korea (NRF) grant and National Research Council of Science & Technology (NST) grant funded by the Korean government (MSIT) [grant numbers 2021M2E2A2081061, CAP-20-03-KAERI].

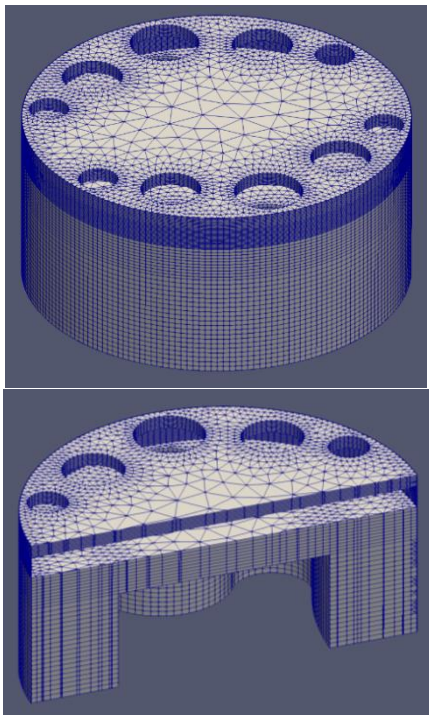

Fig. 4. Full grid system (top) and half region (bottom) of computational domain

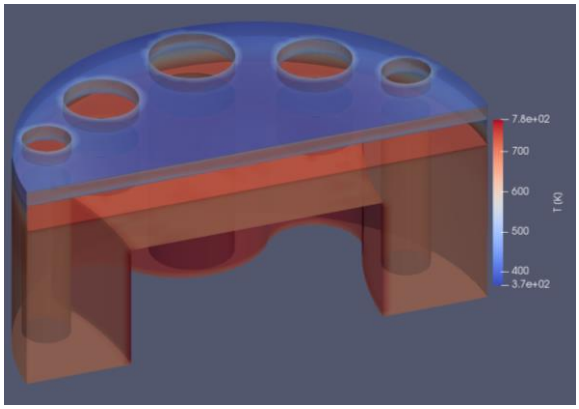

Fig. 5. Temperature distribution

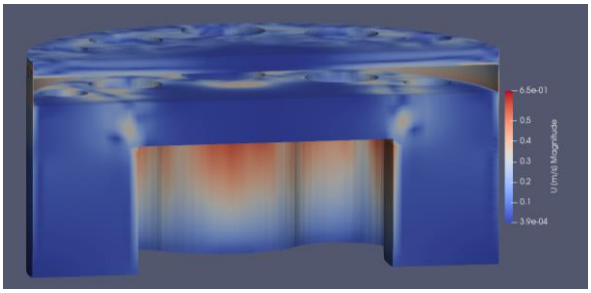

Fig. 6. Velocity distribution

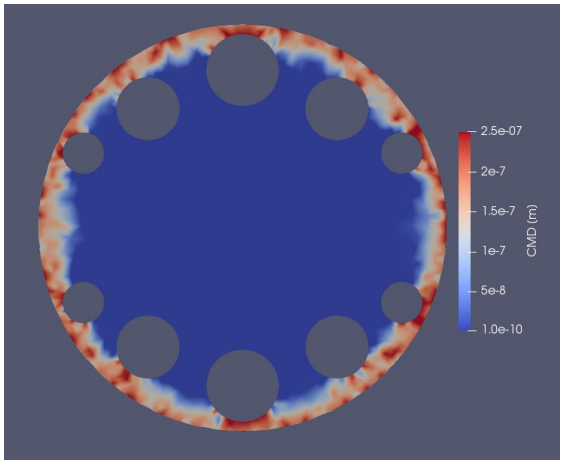

Fig. 7. Counter mean diameter at a horizontal section

REFERENCES

[1] H. Ohira, Numerical Simulation of Aerosol Behavior in Turbulent Natural Convection, Journal of Nuclear Science and Technology, Vol.39, pp.743-751, 2002.
[2] E. Frederix, Eulerian Modeling of Aerosol Dynamics, PhD Thesis, University of Twente, 2016.
[3] L. Talbot, R.K. Cheng, R.W. Schefer and D.R. Willis, Thermophoresis of Particles in a Heated Boundary Layer, Journal of Fluid Mechanics, Vol.101, pp.737-758, 1980.
[4] M. Hortmann, M. Peric and G. Scheuerer, Finite Volume Multigrid Prediction of Laminar Natural Convection: Benchmark Solution, International Journal for Numerical Methods in Fluids, Vol.11, pp.189-207, 1990.
[5] S. Yeom, J.W. Han, S. Ryu, D. Kim, J.H. Eoh and S.R. Choi, Design and Evaluation of Reactor Vault Cooling System in PGSFR, Nuclear Engineering and Design, Vol.365, pp.110717, 2020.